EUROPEAN ORGANISATION FOR NUCLEAR RESEARCH

CERN-EP/90-55
APRIL 30, 1990

The OPAL Collaboration

Evidence for Final State Photons in Multihadronic Decays of the Z^0

M.Z. Akrawy[11], G. Alexander[21], J. Allison[14], P.P. Allport[5], K.J. Anderson[8], J.C. Armitage[6], G.T.J. Arnison[18], P. Ashton[14], G. Azuelos[16,f], J.T.M. Baines[14], A.H. Ball[15], J. Banks[14], G.J. Barker[11], R.J. Barlow[14], J.R. Batley[5], J. Becker[9], T. Behnke[7], K.W. Bell[18], G. Bella[21], S. Bethke[10], O. Biebel[3], U. Binder[9], I.J. Bloodworth[1], P. Bock[10], H. Breuker[7], R.M. Brown[18], R. Brun[7], A. Buijs[7], H.J. Burckhart[7], P. Capiluppi[2], R.K. Carnegie[6], A.A. Carter[11], J.R. Carter[5], C.Y. Chang[15], D.G. Charlton[7], J.T.M. Chrin[14], I. Cohen[21], W.J. Collins[5], J.E. Conboy[13], M. Couch[1], M. Coupland[12], M. Cuffiani[2], S. Dado[20], G.M. Dallavalle[2], P. Debu[19], M.M. Deninno[2], A. Dieckmann[10], M. Dittmar[4], M.S. Dixit[17], E. Duchovni[24], I.P. Duerdoth[7,d], D. Dumas[6], H. El Mamouni[16], P.A. Elcombe[5], P.G. Estabrooks[6], E. Etzion[21], F. Fabbri[2], P. Farthouat[19], H.M. Fischer[3], D.G. Fong[15], M.T. French[18], C. Fukunaga[22], A. Gaidot[19], O. Ganel[24], J.W. Gary[10], J. Gascon[16], N.I. Geddes[18], C.N.P. Gee[18], C. Geich-Gimbel[3], S.W. Gensler[8], F.X. Gentit[19], G. Giacomelli[2], V. Gibson[5], W.R. Gibson[11], J.D. Gillies[18], J. Goldberg[20], M.J. Goodrick[5], W. Gorn[4], D. Granite[20], E. Gross[24], P. Grosse-Wiesmann[7], J. Grunhaus[21], H. Hagedorn[9], J. Hagemann[7], M. Hansroul[7], C.K. Hargrove[17], J. Hart[5], P.M. Hattersley[1], M. Hauschild[7], C.M. Hawkes[7], E. Heflin[4], R.J. Hemingway[6], R.D. Heuer[7], J.C. Hill[5], S.J. Hillier[1], C. Ho[4], J.D. Hobbs[8], P.R. Hobson[23], D. Hochman[24], B. Holl[7], R.J. Homer[1], S.R. Hou[15], C.P. Howarth[13], R.E. Hughes-Jones[14], P. Igo-Kemenes[10], H. Ihssen[10], D.C. Imrie[23], A. Jawahery[15], P.W. Jeffreys[18], H. Jeremie[16], M. Jimack[7], M. Jobes[1], R.W.L. Jones[11], P. Jovanovic[1], D. Karlen[6], K. Kawagoe[22], T. Kawamoto[22], R.G. Kellogg[15], B.W. Kennedy[13], C. Kleinwort[7], D.E. Klem[17], G. Knop[3], T. Kobayashi[22], T.P. Kokott[3], L. Köpke[7], R. Kowalewski[6], H. Kreutzmann[3], J. von Krogh[10], J. Kroll[8], M. Kuwano[22], P. Kyberd[11], G.D. Lafferty[14], F. Lamarche[16], W.J. Larson[4], M.M.B. Lasota[11], J.G. Layter[4], P. Le Du[19], P. Leblanc[16], A.M. Lee[15], D. Lellouch[7], P. Lennert[10], L. Lessard[16], L. Levinson[21], S.L. Lloyd[11], F.K. Loebinger[14], J.M. Lorah[15], B. Lorazo[16], M.J. Losty[17], J. Ludwig[9], N. Lupu[20], J. Ma[4,b], A.A. Macbeth[14], M. Mannelli[7], S. Marcellini[2], G. Maringer[3], A.J. Martin[11], J.P. Martin[16], T. Mashimo[22], P. Mättig[7], U. Maur[3], T.J. McMahon[1], A.C. McPherson[6,c], F. Meijers[7], D. Menszner[10], F.S. Merritt[8], H. Mes[17], A. Michelini[7], R.P. Middleton[18], G. Mikenberg[24], D.J. Miller[13], C. Milstene[21], M. Minowa[22], W. Mohr[9], A. Montanari[2], T. Mori[22], M.W. Moss[14], P.G. Murphy[14], W.J. Murray[5], B. Nellen[3], H.H. Nguyen[8], M. Nozaki[22],

A.J.P. O'Dowd[14], S.W. O'Neale[7,e], B.P. O'Neill[1], F.G. Oakham[17], F. Odorici[2], M. Ogg[6], H. Oh[4], M.J. Oreglia[8], S. Orito[22], J.P. Pansart[19], G.N. Patrick[18], S.J. Pawley[14], P. Pfister[9], J.E. Pilcher[8], J.L. Pinfold[24], D.E. Plane[7], B. Poli[2], A. Pouladdej[6], T.W. Pritchard[11], G. Quast[7], J. Raab[7], M.W. Redmond[8], D.L. Rees[1], M. Regimbald[16], K. Riles[4], C.M. Roach[5], S.A. Robins[11], A. Rollnik[3], J.M. Roney[8], S. Rossberg[9], A.M. Rossi[2,a], P. Routenburg[6], K. Runge[9], O. Runolfsson[7], S. Sanghera[6], R.A. Sansum[18], M. Sasaki[22], B.J. Saunders[18], A.D. Schaile[9], O. Schaile[9], W. Schappert[6], P. Scharff-Hansen[7], H. von der Schmitt[10], S. Schreiber[3], J. Schwarz[9], A. Shapira[24], B.C. Shen[4], P. Sherwood[13], A. Simon[3], G.P. Siroli[2], A. Skuja[15], A.M. Smith[7], T.J. Smith[1], G.A. Snow[15], E.J. Spreadbury[13], R.W. Springer[15], M. Sproston[18], K. Stephens[14], H.E. Stier[9], R. Ströhmer[10], D. Strom[8], H. Takeda[22], T. Takeshita[22], T. Tsukamoto[22], M.F. Turner[5], G. Tysarczyk-Niemeyer[10], D. Van den plas[16], G.J. VanDalen[4], G. Vasseur[19], C.J. Virtue[17], A. Wagner[10], C. Wahl[9], C.P. Ward[5], D.R. Ward[5], J. Waterhouse[6], P.M. Watkins[1], A.T. Watson[1], N.K. Watson[1], M. Weber[10], S. Weisz[7], N. Wermes[10], M. Weymann[7], G.W. Wilson[7], J.A. Wilson[1], I. Wingerter[7], V-H. Winterer[9], N.C. Wood[13], S. Wotton[7], B. Wuensch[3], T.R. Wyatt[14], R. Yaari[24], Y. Yang[4,b], G. Yekutieli[24], T. Yoshida[22], W. Zeuner[7], G.T. Zorn[15],

[1]School of Physics and Space Research, University of Birmingham, Birmingham, B15 2TT, UK
[2]Dipartimento di Fisica dell' Università di Bologna and INFN, Bologna, 40126, Italy
[3]Physikalisches Institut, Universität Bonn, D-5300 Bonn 1, FRG
[4]Department of Physics, University of California, Riverside, CA 92521 USA
[5]Cavendish Laboratory, Cambridge, CB3 0HE, UK
[6]Carleton University, Dept of Physics, Colonel By Drive, Ottawa, Ontario K1S 5B6, Canada
[7]CERN, European Organisation for Particle Physics, 1211 Geneva 23, Switzerland
[8]Enrico Fermi Institute and Department of Physics, University of Chicago, Chicago Illinois 60637, USA
[9]Fakultät für Physik, Albert Ludwigs Universität, D-7800 Freiburg, FRG
[10]Physikalisches Institut, Universität Heidelberg, D-6900 Heidelberg, FRG
[11]Queen Mary and Westfield College, University of London, London, E1 4NS, UK
[12]Birkbeck College, London, WC1E 7HV, UK
[13]University College London, London, WC1E 6BT, UK
[14]Department of Physics, Schuster Laboratory, The University, Manchester, M13 9PL, UK
[15]Department of Physics and Astronomy, University of Maryland, College Park, Maryland 20742, USA
[16]Laboratoire de Physique Nucléaire, Université de Montréal, Montréal, Quebec, H3C 3J7, Canada
[17]National Research Council of Canada, Herzberg Institute of Astrophysics, Ottawa, Ontario K1A 0R6, Canada
[18]Rutherford Appleton Laboratory, Chilton, Didcot, Oxfordshire, OX11 0QX, UK
[19]DPhPE, CEN Saclay, F-91191 Gif-sur-Yvette, France
[20]Department of Physics, Technion-Israel Institute of Technology, Haifa 32000, Israel
[21]Department of Physics and Astronomy, Tel Aviv University, Tel Aviv 69978, Israel
[22]International Centre for Elementary Particle Physics and Dept of Physics, University of Tokyo, Tokyo 113, and Kobe University, Kobe 657, Japan

[23]Brunel University, Uxbridge, Middlesex, UB8 3PH UK
[24]Nuclear Physics Department, Weizmann Institute of Science, Rehovot, 76100, Israel

[a]Present address: Dipartimento di Fisica, Università della Calabria, 87036 Rende, Italy
[b]On leave from Harbin Institute of Technology, Harbin, China
[c]Now at Applied Silicon Inc
[d]On leave from Manchester University
[e]On leave from Birmingham University
[f]and TRIUMF, Vancouver, Canada

(Submitted to Phys. Lett.)

Abstract

From the observed yield and properties of isolated energetic photons in the reaction $e^+e^- \to Z^0 \to hadrons + \gamma$ measured with the OPAL detector at LEP, evidence for final state radiation from primary quarks is obtained. Combined with the measurement of the total hadronic width of the Z^0, the observed rate allows the extraction of the electroweak coupling constants of up and down type quarks:

$$v_{1/3}^2 + a_{1/3}^2 = 1.24 \pm 0.44 \quad \text{and} \quad v_{2/3}^2 + a_{2/3}^2 = 1.72 \pm 0.64$$

No evidence for additional photon production from anomalous decays of the Z^0 or from decays of new particles is found. This measurement limits the contribution to the total Z^0 width from such sources to be less than 8.2 MeV at the 95% confidence level.

1 Introduction

This paper presents a measurement of isolated, energetic photon production in the reaction $e^+e^- \rightarrow Z^0 \rightarrow hadrons + \gamma$. In multihadronic events, prompt, high energy photons are expected to arise from initial and final state bremsstrahlung.

In this analysis the yield and properties of isolated photons are found to be consistent with the expectation for final state photon radiation from quarks. The measurement is used to determine the weak couplings of up and down type quarks and to search for Z^0 decays beyond the Standard Model. The amount of final state radiation should be proportional to the squares of the electric charges of the produced quarks [1]. Thus, a selection of events with final state radiation will enrich the proportion of charge 2/3 quarks. In conjunction with the measured hadronic width, the rate of final state radiation allows the determination of the electroweak couplings of up and down type quarks [2].

Events with isolated, energetic photons may also indicate new processes, such as new particle production or anomalous decays of the Z^0. Examples of new particles with this signature are a fourth generation, charge 1/3 quark that is lighter than the third generation top quark [3], or an excited quark. If the Z^0 boson is formed from constituents, its decay into photons could provide the first evidence of its substructure [4].

2 The OPAL Detector

This analysis is based on an integrated luminosity of about 1.3 pb^{-1} collected with the OPAL detector [5] at LEP. The data were recorded at center-of-mass energies E_{cm} between 88.28 and 95.04 GeV around the Z^0 pole. The basic triggers and detector components for the detection of multihadronic events are discussed in [6].

Of particular importance to this study are the main central drift chamber and the barrel part of the electromagnetic calorimeter. The cylindrical drift chamber, which is four meters in length and two meters in radius, provides a measurement of the momenta of charged particles over almost the entire solid angle in a magnetic field of 4.326 kG. Each particle track is measured by up to 159 layers of wires at radii in the range 25.5 cm to 184.5 cm from the beam axis. The current single hit resolution is measured to be 140 μm in the plane transverse to the beam and 6.5 cm along the direction of the beam.

The barrel electromagnetic calorimeter, covering the solid angle $|cos\theta| \leq 0.82$, where θ is the polar angle with respect to the beam direction, consists of 9440 lead glass blocks of 24.6 radiation lengths, pointing towards the interaction region and each subtending an angular region of approximately 40x40 $mrad^2$. Blocks are slightly tilted from a perfect pointing geometry to prevent photons from escaping through inter-block gaps. With the material in front and the current uncertainty of the gain calibration, the effective energy resolution is about 5% for 10 GeV and 3% for 45 GeV electrons. The position resolution is better than $\delta\theta, \delta\phi = 5$ mrad in the polar and azimuthal angles for showers of more than 10 GeV energy.

The hadron calorimeter, consisting of nine limited streamer tube planes within the iron return yoke of the magnet, is located directly behind the electromagnetic calorimeter. In this analysis it is used to check the hadronic background to the isolated photon candidates. The hadron calorimeter was operational for approximately 85% of the data used.

A final check on photon identity is provided by the presampler, which is a cylindrical array of 16 double planed chambers, also containing limited streamer tubes, with both wire and cathode strip readout. The presampler modules are mounted on the outside of the coil, in front of the lead glass array, and cover the entire barrel region. Photons, unlike neutral hadrons, are likely to initiate electromagnetic showers when passing through the coil and pressure vessel; both the amplitude and position of these showers are measured by the presampler.

3 The Selection of Multihadronic Events with Photons

The hadron selection is based on the central jet chamber and the electromagnetic barrel calorimeter [6]. Multihadronic events are required to have at least five well measured tracks and more than seven clusters in the electromagnetic calorimeter. An accepted track, reconstructed from at least 20 hits in the main drift chamber, must have a minimum transverse momentum to the beam of 250 MeV, a reconstructed distance of closest approach to the beam axis of less than 5 cm, and a longitudinal displacement along the beam direction from the nominal interaction point of less than 30 cm at the point of closest approach to the beam. A cluster in the lead glass calorimeter consists of at least two adjacent blocks with a total energy of more than 100 MeV. The energy sum of all accepted clusters must exceed 11% of the e^+e^- centre-of-mass energy. 27,309 events satisfy these requirements. The acceptance for multihadronic events is estimated to be 98%. The background from beam-gas events, τ pair production, two-photon production and other processes is less than 0.5%.

Isolated photon candidates must lie in a fiducial region of $|\cos\theta| \leq 0.72$ and must have an energy of at least 10 GeV. Isolation requirements are that no tracks and no other electromagnetic clusters occur within a cone of half angle 20 degrees centered on the photon direction: 69 events have such an isolated photon candidate.

Background from neutral hadrons and from photons due to π^0 decays are further suppressed by requiring that the shape of the electromagnetic cluster be consistent with that expected from a single photon:

1. The cluster consist of no more than 15 lead glass blocks.
2. The width of the cluster, defined by

$$M^{EB} = \sqrt{\frac{\Sigma E_i \cdot ((\phi_i - <\phi>)^2 + (\theta_i - <\theta>)^2)}{\Sigma E_i}},$$

be less than 25 mrad, where ϕ_i and θ_i are the polar and azimuthal angles of each block i in the cluster and E_i is the energy deposited in the block; $<\phi>$ and $<\theta>$

describe the centroid of the cluster, and the summation runs over all blocks in the cluster.

3. The sharing of energy among the blocks must be consistent with that expected from a photon. For this purpose $C = \frac{1}{N_{Blocks}} \cdot \min \sum \frac{(E_i^{exp}(\theta,\phi) - E_i^{obs})^2}{\sigma_i^2}$ is calculated for each cluster, where E_i^{exp}, E_i^{obs} and σ_i^2 denote the expected energy, observed energy and its variance for block i, respectively. The summation is over all blocks of the cluster. The expected energy E_i^{exp}, a function of the incident photon angles θ and ϕ, is calculated by integrating the 3-dimensional standard shower profile function over a block. The incident angles θ and ϕ are chosen to minimize the summation: C is then required to be less than 1.5.

All these conditions are satisfied by 44 events. The points in figs. 1 a-b show the distributions of the number of blocks and the width M^{EB} of the shower before the requirements 1 to 3 are imposed. In fig. 1c the distribution of the cluster shape parameter C is shown after cuts 1 and 2 and for $p_T \geq 5$ GeV where p_T is the transverse momentum of the cluster with respect to the thrust axis (see below).

The efficiency for selecting high energy electromagnetic clusters was determined from a reference sample of unambiguous photons collected during the same running period. Photons from radiative lepton-pair events and the process $e^+e^- \rightarrow \gamma\gamma$ [7] were selected. The distributions from this sample are also displayed in figs. 1a-c. The photon candidates from multihadronic events exhibit tails in these distributions which are rejected by the selection criteria. Within the selected region the distributions of the candidates are consistent with those of the reference sample. These requirements are found to retain 91% of genuine photons. An additional loss of 7% arises from photon conversion before or inside the tracking chamber. The efficiency for photon identification is thus estimated to be 84±4%. The variation of the photon identification efficiency with energy and polar angle is less than ±2%. Losses due to noise induced clusters falling within the isolation cone are less than 0.1%, which were calculated using electron pair events.

To suppress photons from highly energetic neutral pions, which predominantly occur within the jets, an additional cut on the transverse momentum p_T of the photon relative to the thrust axis of $p_T > 5$ GeV was applied. The thrust axis has been calculated with all particles including the photon: 35 events survived all these cuts.

All of the 35 selected events with an isolated, energetic electromagnetic cluster have been identified as being multihadronic by a visual scan. A typical event is displayed in fig. 2. Jets with a total of 18 good tracks and energy in the lead glass and the hadron calorimeter can be seen. The isolated photon is at the right.

4 Background Contributions from Fragmentation Remnants

The remaining background to the observed candidate events, due to fragmentation remnants, is estimated in two steps. In a first step, the predictions of Monte Carlo simulations are studied and compared with the data. Secondly, the experimental event sample itself is used to estimate the background.

First, hadronic events without final state photons were simulated. Two different hadronization schemes as implemented in the LUND QCD shower program [8] and the HERWIG program [9], folded with initial state radiation of $O(\alpha)$ [10] were used to generate hadronic events. These were then passed through a detailed simulation of the OPAL detector [11]. The predictions from both hadronization schemes are in good agreement. When normalized to the multihadronic data sample and after the same event and photon selections as described above, both simulations predict 1.2±1.6 events due to hadron background. This number is significantly smaller than the number of observed photon candidates. The simulation indicates that the background is almost entirely due to isolated π^0's. Other background sources yielding one neutral cluster, such as η's or overlaps of several particles due to decays of the type $K^{*0} \rightarrow \pi^0 K^0_L$, are eliminated by the cluster shape requirement (3).

In the second step several independent methods were used to estimate the background from the data directly:

- (i) Since, for energies below 30 GeV, a photon and the potential background from π^0's and overlapping neutral hadrons have different distributions in the cluster shape parameter C, the observed distribution was used to unfold these contributions.
- (ii) Assuming the background from fragmentation is due only to π^0's, approximate isospin symmetry can be invoked to obtain upper limits for the background from the yield of isolated charged particles.
- (iii) Additional detector components, the hadron calorimeter and the presampler, provide independent corroboration of photon identification.

The various methods lead to the following direct background estimates from the data.

- (i) For cluster energies of less than $\sim$ 30 GeV the cluster shape analysis (selection 3 above) allows one to discriminate statistically π^0's from single γ's. Shown in figure 1d are the measured distributions in C and those expected for genuine photons and for π^0's of energies between 10 and 30 GeV. The two distributions overlap, but are different. Above 30 GeV, however, photons and π^0's are hardly distinguishable. To estimate the contribution of γ's in the region of $C \leq 1.5$, the cluster shape range was split into intervals of 0-0.5, 0.5-1, 1-1.5, 1.5-4, and larger than 4. In these intervals the measured distribution was expanded into a linear equation system with the numbers of γ's, π^0's and neutral hadrons ($N^\gamma, N^{\pi^0}, N^{nh}$) as free parameters:

$$N_i^{obs} = p_i^\gamma \cdot N^\gamma + p_i^{\pi^0} \cdot N^{\pi^0} + p_i^{nh} \cdot N^{nh}$$

The p_i^c denote the fraction of particle type c in the interval i. The agreement of the simulation of these shower shapes with the data was checked using the reference photon sample described above. Since the agreement was very good, and to increase the statistics, the p_i^c were taken from the Monte Carlo simulation. The linear equation systems were solved for the two energy regions of 10 - 20 and 20 - 30 GeV, yielding a total background contribution of 8.4±3.8 and 1.9±3.0 respectively. The fit result is displayed for the γ and π^0 component in fig. 1d. For energies above 30 GeV, corresponding to 17% of the candidates, the C distribution is consistent with being due to a photon, but a discrimination against π^0 background is not possible. Assuming the same background fraction as for lower energies yields another 1.8±3.0 events. With this method we obtained a total of 12.1±5.7 events from the fragmentation background.

For the interval $C \leq 1.5$, used for the final photon sample, the corresponding numbers for the the three energy regions are 3.5±1.4, 1.1±1.8 and 0.9±1.4 respectively, yielding a total of 5.5±2.7 background events.

- (ii) Charged pions have been measured to occur about twice as often as neutral pions (for a review of particle yields at lower center-of-mass energies see [12]). Hence charged particles were subjected to the same criteria as the isolated neutral clusters. From a subsample of 15,687 events five candidates for isolated charged tracks were found. This implies an upper limit on the background due to π^0's of 4.4±2.0, normalized to the overall event yield. Note that charged kaons and protons too are considered and therefore the background contribution is overestimated. Most of the tracks had energies close to 10 GeV.

  This argument becomes more complicated if the limited granularity of the electromagnetic calorimeter is taken into account. Before selection 3 the separation of two neutral clusters is 80 mrad. For a charged particle analysis, taking this granularity into account, the number of charged jets is expected to exceed the number of neutral jets by more than a factor 2 (the Monte Carlo simulations predict about a factor three for 80 mrad separation). Allowing several particles in a cone of half opening angle of 80 mrad, instead of one isolated particle, yields an additional 13 events or an expected background contribution of less than 11.3±3.2 events. In total, *less* than 15.7±3.8 events from fragmentation remnants are expected to contribute to the photon candidates. This number is the background *before* the cut in C.

  This estimate is consistent with that obtained from the cluster shape analysis.

- (iii) Additional detector components were used to establish the consistency with the photon assignment. For 86% of all photon candidates the hadron calorimeter was operational. Only two of the 35 candidates have more than 1 GeV of energy deposited there. Such large energy deposition exceeds the expectation for genuine γ's and can only be explained with a hadronic component of the cluster. This number is consistent with the background expectation given above.

  The presampler signals of these photon candidates have been compared to the reference data sample for genuine photons. The distributions are the same within statistical error; both means and sigmas of the distributions agree to within 5%. The differences in positions between the presampler and lead glass clusters also agree, in both cases giving a sigma of about 10 mrad, or 1/4 of the angle subtended by a lead glass block.

In summary, the contribution from fragmentation remnants to the candidate sample was estimated by different methods without reference to a fragmentation model. All these checks yield consistent numbers. For the further analysis those from the cluster shape analysis were assumed giving 5.5±3.0 events, where the error takes into account the statistical and systematic uncertainties of the procedures.

5 Evidence for Final State Photon Radiation

Besides the fragmentation remnants, initial state radiation is a background to the final state photon sample. The Monte Carlo simulations predict a contribution of 1.8±0.5 events from initial state radiation. This leaves 27.7±6.2 events due to additional sources. The most natural explanation is photon emission from quarks. A simulation of final state bremsstrahlung in hadronic events [13] predicts a contribution of 21.6±1.5 additional photons, consistent with the measured yield. The expected contributions and the observed yield are listed in table 1.

For these numbers fragmentation parameters optimized to describe the measured event shape distributions have been used [14]. As discussed in [2], uncertainties in these parameters, especially in the QCD scale parameter Λ_{QCD} affect the predicted yield of photons. The value of Λ_{QCD}, used in the leading log approximation of the parton evolution, has been determined from a comparison of the Monte Carlo prediction to the measured event shapes at center of mass energies around 30 GeV and at Z^0 energies. The values obtained are between 290 and 420 MeV. For the following discussion, a conservatively wide range of $150 \leq \Lambda_{QCD} \leq 600$ MeV will be assumed, corresponding to an additional uncertainty on the number of final state photons of ± 2.8 events.

To establish further the evidence for final state photons, the measured kinematical distributions are compared with the expectation. The distribution of the transverse momentum with respect to the thrust axis is shown in fig. 3a before applying the p_T cut of 5 GeV. The spectrum extends up to $p_T > 20$ GeV. The expected shape from final state radiation reproduces the data well. The p_T cut of 5 GeV leads to a loss of final state photons of 12%. The energy spectrum for photons with $p_T > 5$ GeV and the expected fragmentation background are displayed in fig. 3b. The measured spectrum agrees well with the one expected from final state bremsstrahlung. The dashed line shows the energy spectrum of all hadrons. The photon spectrum is much harder than the hadron spectrum, as expected for photons emitted before hadronization.

Thus, both the overall yield and the kinematical distributions of the photons provide evidence for final state bremsstrahlung. This measurement supplements earlier results from e^+e^- experiments at center-of-mass energies near 30 GeV [15].

6 Determination of the Quark Couplings

Photons possessing large transverse momenta with respect to the quark direction are radiated directly from the primary quarks in Z^0 decays [16]. For the selection criteria applied, Monte Carlo studies predict that less than 10^{-3} photons are due to secondary quarks. The yield of the selected photons therefore measures directly the electric charges of the primary quarks.

If all observed photons are attributed to standard model sources, the electroweak couplings of charge 1/3 and 2/3 quarks can be determined from this measurement, in conjunction with the observed hadronic width of the Z^0 [2]. We assume the same production rate for all 1/3 charged quarks and for all 2/3 charged quarks, respectively. The weak couplings are denoted by

$$c_i \;=\; v_i^2 \;+\; a_i^2 \tag{1}$$

with the standard model notation

$$v_i \;=\; 2 \cdot I_{3,i} - 4 \cdot Q_i \cdot \sin^2\theta_w \quad \text{and} \quad a_i \;=\; 2 \cdot I_{3,i} \tag{2}$$

where i indexes 1/3 or 2/3 charged quarks, v and a are the vector and axial couplings, and I_3, Q, and θ_w are the third weak isospin component, the charge of the quarks and the weak mixing angle, respectively. The hadronic decay width of the Z^0 for the known five flavors is in first order QCD

$$\Gamma_{had} \;=\; N_c \frac{G_\mu \cdot M_Z^3}{24 \cdot \pi\sqrt{2}} \cdot \left(1 \;+\; \frac{\alpha_s}{\pi}\right) \cdot (3 \cdot c_{1/3} \;+\; 2 \cdot c_{2/3}). \tag{3}$$

Here N_c is the number of colors, G_μ the Fermi coupling constant at the muon mass, M_Z the mass of the Z^0 , and α_s the strong coupling constant.

Because the photons couple with the square of the electric charge of the quarks, the proportion of u type quarks is enhanced by a factor of four relative to the d type quarks in the radiative width. The yield of radiative events is therefore proprotional to $(3 \cdot c_{1/3} + 8 \cdot c_{2/3})$. To extract these couplings from the data, the observed yield was normalized to the expectation in the Monte Carlo. This procedure takes into account the limited acceptance due to the cuts applied.

$$(N_{\gamma q\bar{q}})_{exp} \;=\; \frac{(N_{\gamma q\bar{q}})_{MC}}{(3 \cdot c_{1/3} + 8 \cdot c_{2/3})_{MC}} \cdot (3 \cdot c_{1/3} + 8 \cdot c_{2/3})_{exp} \tag{4}$$

The indices 'exp' and 'MC' stand for either the experimental values or those obtained from the simulation [13]. The number of events after selection and including inefficiencies in the photon detection is denoted by $(N_{\gamma q\bar{q}})_{exp}$; $(N_{\gamma q\bar{q}})_{MC}$ is the number of events predicted by the Monte Carlo, normalized to the observed luminosity. Dominant systematic errors affecting this relation are due to uncertainties in the background subtraction (8.6%), to the simulation of the photon detection efficiency (4%), and to the uncertainty in the fragmentation modeling (8.0%). Higher order QCD corrections are effectively accounted for by the parton shower algorithm implemented in the Monte Carlo. The systematic errors are smaller than the statistical error. For the large-p_T photons considered in this analysis the theoretical uncertainty on the expected photon spectrum is small [17].

The measurement of the hadronic width and mass of the Z^0 [18] together with the yield of final state bremsstrahlung thus allows one to solve equations 3 and 4 for $c_{1/3}$ and $c_{2/3}$. Assuming all 27.7±6.2 (statistical and systematic error) photons observed for $p_T \geq 5$ GeV are due to final state radiation, yields

$$c_{1/3} = v_{1/3}^2 + a_{1/3}^2 = 1.24 \pm 0.44 \text{ and } c_{2/3} = v_{2/3}^2 + a_{2/3}^2 = 1.72 \pm 0.64.$$

This is in agreement with the standard model prediction of $c_{1/3} = 1.48$ and $c_{2/3} = 1.15$ for $\sin\theta_w^2 = 0.229$. The somewhat larger value for $c_{2/3}$ and lower value for $c_{1/3}$ reflects the larger than expected photon yield, implying a larger contribution from charge 2/3 quarks. These results, together with the 1 σ intervals from the hadronic width, measured with the same data, and the number of final state bremsstrahlung photons, are depicted in fig. 4. They agree with the results obtained by combining measurements from several e^+e^- experiments at lower energies [19] and with the expectations of the standard model (black point). Variations of Λ_{QCD} between 150 and 600 MeV in the model calculations lead to shifts for $c_{1/3}$ of (+0.20,-0.32) and for $c_{2/3}$ of (-0.36,+0.44).

7 Limits on New Processes

The absence of any significant excess of isolated photons in the data over that expected from the standard model, including initial and final state bremsstrahlung, allows limits to be placed on the existence of new phenomena. To increase the sensitivity to possible new processes, only events with $p_T \geq 10$ GeV were considered; 24 events are observed in this region, where 17.9 are expected. To take into account the uncertainties in the background estimate and in the fragmentation process, a conservative approach was adopted: no background from fragmentation remnants was assumed, and in addition, Λ_{QCD} was assumed to be 600 MeV, yielding the minimum expected number of photons for the Λ_{QCD} range considered. This reduces the expected number of events to 14.8. It implies that other processes are allowed to contribute at most 19.0 events with 95% confidence level [20]. New particles considered in this analysis are: a) a fourth generation charge 1/3 quark (b') decaying into a photon and a bottom quark; and b) an excited quark (q^*) decaying into a photon and a normal quark (q). The possibility that the Z^0 is composite and decays into a photon and hadronic matter is also explored. For all cases the branching ratio to photons is model dependent.

For the selection criteria applied, the acceptance for the production and decay of these particles was determined from a Monte Carlo simulation based on the LUND QCD showering algorithm.

For masses of the b' quark in the range from 30 GeV to the kinematic limit we find that, depending on the b' mass, between 38% and 31% of all photons from b' decays are retained by our event selection, giving:

$$\frac{\Gamma(Z^0 \to b' + \bar{b}')}{\Gamma(Z^0 \to hadrons)} \cdot BR(b' \to \gamma + X) \leq 0.0022 \qquad (5)$$

at the 95% confidence level. Fig. 5 shows the limit on the branching ratio, $b' \to \gamma + X$, for different masses of the b', assuming standard coupling to the Z^0 and taking into account the threshold factors [1].

An excited quark could be produced with much larger masses, namely $M_{q^*} \leq M_Z - M_{\bar{q}}$ in $Z^0 \to q^*\bar{q}$. The acceptance for photonic decays falls from 27% at a mass of 55 GeV to 25% at 65 GeV. As the mass increases, the direction of the thrust axis becomes more aligned with the direction of the energetic photon and consequently the acceptance decreases because of the cut on p_T at 10 GeV. On the other hand, the kinematically allowed range of the photon energy, E_γ, becomes more restricted. Therefore, for $M_{q^*} \geq 55$ GeV the cut on p_T was replaced by the requirement that $17 \leq E_\gamma \leq 24$ GeV. In this case, exclusion with 95% confidence level requires an expectation greater than 8.6 signal events. The resulting acceptance ranges from 8% at an M_{q^*} of 55 GeV to 59% at 85 GeV, and the limit for the product of the branching ratios is 0.0037 for $M_{q^*} = 55$ GeV and 0.0006 for $M_{q^*} = 85$ GeV.

The partial width for Z^0 decay into a q^* depends on several unknown parameters; the coupling strength f, the composite scale Λ_c^* and the chiral structure (c, d) of the magnetic dipole couplings [4]. For $f(c^2 + d^2)/\Lambda_c^{*2}$ equal to $1/100^2$ GeV^{-2}, fig. 5 shows the resulting limits on the branching ratio $q^* \to \gamma + X$ as a function of the q^* mass.

These results exclude the production of these new types of quarks over most of the kinematically available range, even for low branching ratios into photons. The mass range for the b' excluded by this analysis is slightly higher than previous limits obtained [23]. The limits on an excited quark, q^*, depend strongly on the compositeness scale. For instance, for a branching ratio of 10% , theoretically favoured because of the ratio of electromagnetic to strong coupling, and for the couplings assumed in fig 5, the lower limit on the mass is 86 GeV at the 95% confidence level, which significantly extends the limits from previous results [24].

If the Z^0 is composed of charged constituents, it can decay into a photon and hadrons. The possibilities include: a) anomalous three and four boson couplings [25], giving a broad spectrum of photon energies , and b) decay to a scalar partner S, giving nearly monochromatic photons, provided the width is sufficiently small [2].

For case a) the kinematic configurations of the decay are model dependent; for simplicity a three body phase space decay was used. The acceptance for such events, determined by the Monte Carlo simulation with a cut on p_T at 10 GeV is 15%. Using the hadronic width of the Z^0 [18], obtained from the same data, this translates into an upper limit on the partial width of

$$\Gamma(Z^0 \to \gamma + X) \leq 8.2 \text{ MeV}$$

with 95% confidence level.

To search for Z^0 decays to a scalar, case b), the spectrum of the mass recoiling against the isolated photon was studied. Within the experimental resolution, which changes from 3.5 to

[1] The QCD threshold behaviour was taken into account for b' production [21], but was ignored for $q^*\bar{q}$ production. In this case the QCD threshold behaviour depends on the model considered [22].

[2] A small width, equivalent to a small coupling to fermions, could explain the non-observation of such a scalar at lower energies.

0.6 GeV as the recoil mass changes from 32 to 80 GeV, the spectrum exhibits no significant enhancements. For no recoil mass within an interval corresponding to the experimental resolution are there more than four events. Assuming that at most four events originate from the transition leads to the limit $\Gamma(Z^0 \to S + \gamma) \leq 1.9$ MeV with 95% confidence level, for a scalar particle mass range up to 80 GeV. For the model of [26] this excludes scalars of masses $M_S \leq 75$ GeV.

8 Summary

The observed yield of isolated photons with $E_\gamma \geq 10$ GeV and its energy spectrum agree with the expectation for final state bremsstrahlung. This observation is used to establish a new method for determining the quark couplings to the Z^0. From the measurements of the hadronic width of the Z^0 and the observed final state bremsstrahlung, the allowed range for the couplings of up and down type quarks are determined:

$$v_{1/3}^2 + a_{1/3}^2 = 1.24 \pm 0.44 \quad \text{and} \quad v_{2/3}^2 + a_{2/3}^2 = 1.72 \pm 0.64.$$

with additional uncertainties from Λ_{QCD} of about 0.24 and 0.40 respectively.

No evidence for additional sources of prompt photons has been found. With 95% confidence this leads to upper limits on the product branching ratio for a new quark q or for an anomalous decay of the Z^0 into a photon and gluons of

$$\frac{\Gamma(Z^0 \to q + hadrons)}{\Gamma(Z^0 \to hadrons)} BR(q \to \gamma + X) \leq 0.0037 \quad \text{or} \quad \Gamma(Z^0 \to \gamma\, X) \leq 8.2 \text{ MeV}$$

These values exclude the production of new particles and anomalous Z^0 decays over a wide range of parameters.

9 Acknowledgements

This analysis profited from the theoretical advice of various people. We enjoyed discussions with F.Renard, T.Sjöstrand, and P.Zerwas. Their detailed help with Monte Carlo generators and theoretical problems was essential for this analysis.

It is a pleasure to thank the LEP Division for the efficient operation of the machine, the precise information on the absolute energy, and their continuing close cooperation with our experimental group. In addition to the support staff at our own institutions we are pleased to acknowledge the following: The Bundesministerium für Forschung und Technologie, FRG, The Department of Energy, USA, The Institut de Recherche Fondamentale du Commissariat a l'Energie Atomique, The Israeli Ministry of Science, The Minerva Gesellschaft, The National Science Foundation, USA, The Natural Sciences and Engineering Research Council, Canada, The Japanese Ministry of Education, Science and Culture (the Monbusho) and a grant under the Monbusho International Science Research Program, The American Israeli Bi-national

Science Foundation, The Science and Engineering Research Council, UK and The A. P. Sloan Foundation.

References

[1] T.F. Walsh and P. Zerwas, Phys.Lett. *44B* (1973), 195; S.J. Brodsky, C.E. Carlson, and R. Suaya, Phys.Rev.*D14* (1976), 2264; K. Koller, T.F. Walsh, and P. Zerwas, Z.Physik *C2* (1979), 197

[2] P. Mättig and W. Zeuner, paper in preparation

[3] W.S. Hou and R.G. Stuart Phys.Rev.Lett. *62* (1989), 617; Nucl.Phys. *B320* (1989), 277

[4] F. Boudjema et al., in Proceedings of the Workshop on Z - Physics at LEP 1, ed. G. Altarelli, R. Kleiss, and C. Verzegnassi, CERN 89-08

[5] OPAL - collaboration, Technical proposal (1983) and CERN/LEPC/83-4

[6] OPAL - collaboration, M.Z. Akrawy et al., Phys.Lett *231B* (1989), 530

[7] OPAL - collaboration, M.Z. Akrawy et al., CERN-EP/90-29

[8] T. Sjöstrand, Comp. Phys. Comm *39* (1986), 347; JETSET, Version 7.1

[9] G. Marchesini and B.R. Webber, Nucl.Phys. *B310* (1988), 461; HERWIG, Version 3.2

[10] F.A. Berends, R. Kleiss, S. Jadach, Nucl.Phys. *B202* (1982), 63

[11] J. Allison et al., Comp. Phys. Comm. *47* (1987) 55; R. Brun et al., CERN DD/EE/84-1 (1989)

[12] P. Mättig, Phys. Rep. 177 (1989), 141

[13] T. Sjöstrand, JETSET, Version 7.2

[14] OPAL - collaboration, M.Z. Akrawy et al., CERN-EP/90-48

[15] MAC - collaboration, E. Fernandez et al., Phys.Rev.Lett. *54* (1985), 95; JADE - collaboration, W. Bartel et al., Z.Phys. *C28* (1985), 343; TASSO - collaboration, W. Braunschweig et al., Z.Phys. *C41* (1988), 385 JADE - collaboration, D.D. Pitzl et al., preprint DESY 89-129

[16] E. Laermann, T.F. Walsh, I. Schmitt and P.M. Zerwas, Nucl.Phys. *B207* (1982),205

[17] P. Zerwas, private communication

[18] OPAL - collaboration, M.Z. Akrawy et al., CERN-EP/90-27

[19] R. Marshall, Z.Phys. *C43* (1989), 607

[20] Particle Data Group, Phys.Lett. *B204* (1988) pg. 81

[21] T.H. Chang, K.J.F. Gaemers and W.L. van Neerven, Nucl.Phys. *B202* (1982), 407 as implemented in the Monte Carlo program of G. Burgers, LEP CERN 88-06

[22] A.Djouadi, private communication

[23] Mark II collaboration, G.S.Abrams et al., Phys.Rev.Lett. *63* (1989) 2447 OPAL - collaboration, M.Z. Akrawy et al., Phys.Lett *236B* (1990); ALEPH - collaboration, D. Decamp et al., CERN-EP/89-165

[24] CELLO - collaboration, H.J. Behrend et al., Phys.Lett. 181B (1986), 178

[25] F.M. Renard, Phys.Lett. *116B* (1982), 269

[26] F.M. Renard, Phys.Lett. *132B* (1983), 449

FIGURE 1: Electromagnetic cluster shape distributions for the photon candidates in multihadronic events (points) and for the reference photon sample (hashed area) (not normalized, see text) (a) number of lead glass blocks per cluster, (b) width of the cluster, (c) cluster shape variable C. Result of the cluster shape analysis (d) for cluster energies of less than 30 GeV, the lines display the contributions for γ's and π^0's as obtained by the fit (see text).

FIGURE 2: Typical multihadronic event with an isolated photon in the plane transverse to the beam direction. Displayed are the tracks in the central drift chamber and the energy deposition in the lead glass calorimeter. Also shown is the energy deposition in the hadron calorimeter.

FIGURE 3: (a) Transverse momentum with respect to the jet axis: data (points), simulation without final state bremsstrahlung, simulation with fragmentation background plus contribution from final state radiation. (b) Photon energy after a cut in $p_T \geq 5$ GeV. The dashed curve indicates the spectrum of all hadrons plus initial state radiation.

FIGURE 4: Correlation of the couplings for charge 1/3 and 2/3 quarks as obtained from the total hadronic width and from this analysis. Also shown is the expectation from the standard model (black point).

FIGURE 5: Excluded ranges for mass and photonic decay branching ratio at the 95 % confidence for the b' quark and for excited quarks q^*.

Table 1: Observed Photon candidates and expected contributions

	nb. of events
observed yield	35.0 ±5.9
expected fragm. background	5.5±3.0
expected initial state photons	1.8±0.5
Remaining photons	27.7±6.2
expected final state photons	21.6±1.5
uncertainty from fragmentation	±2.8

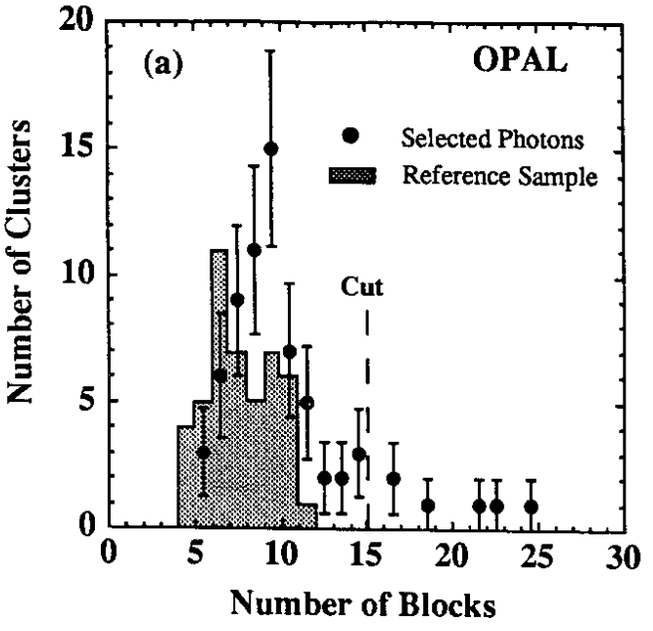
(a)
OPAL
Selected Photons
Reference Sample
Cut
Number of Clusters
Number of Blocks

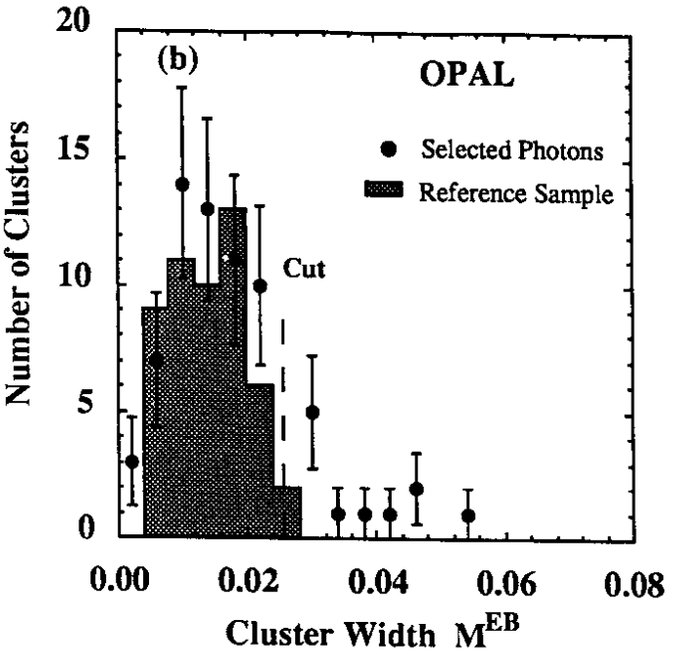
(b)
OPAL
Selected Photons
Reference Sample
Cut
Number of Clusters
Cluster Width M^{EB}

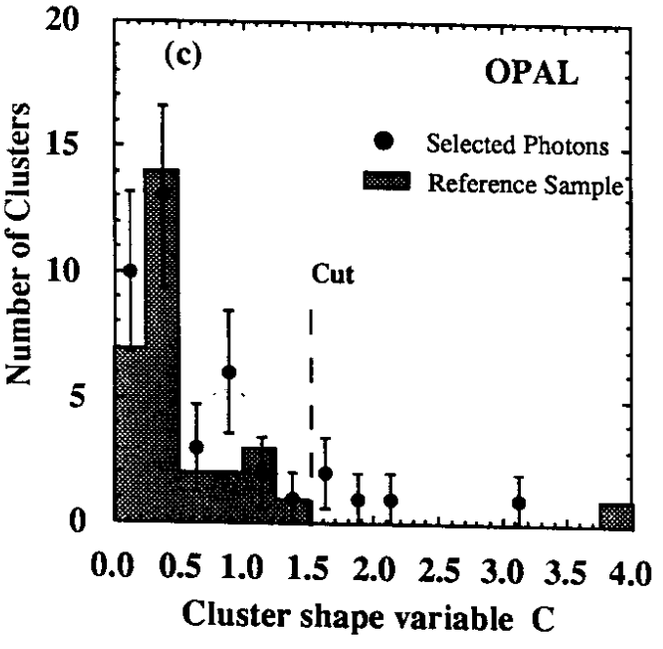
(c)
OPAL
Selected Photons
Reference Sample
Cut
Number of Clusters
Cluster shape variable C

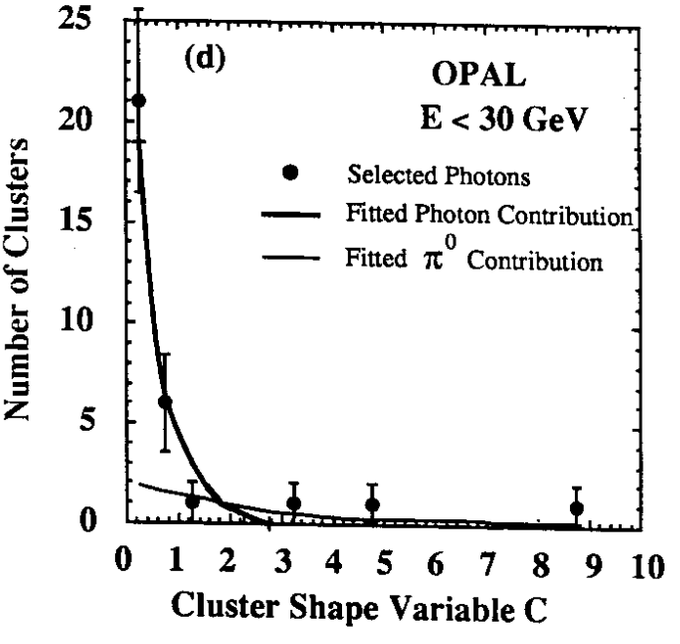
(d)
OPAL
E < 30 GeV
Selected Photons
Fitted Photon Contribution
Fitted π^0 Contribution
Number of Clusters
Cluster Shape Variable C

Figure 1

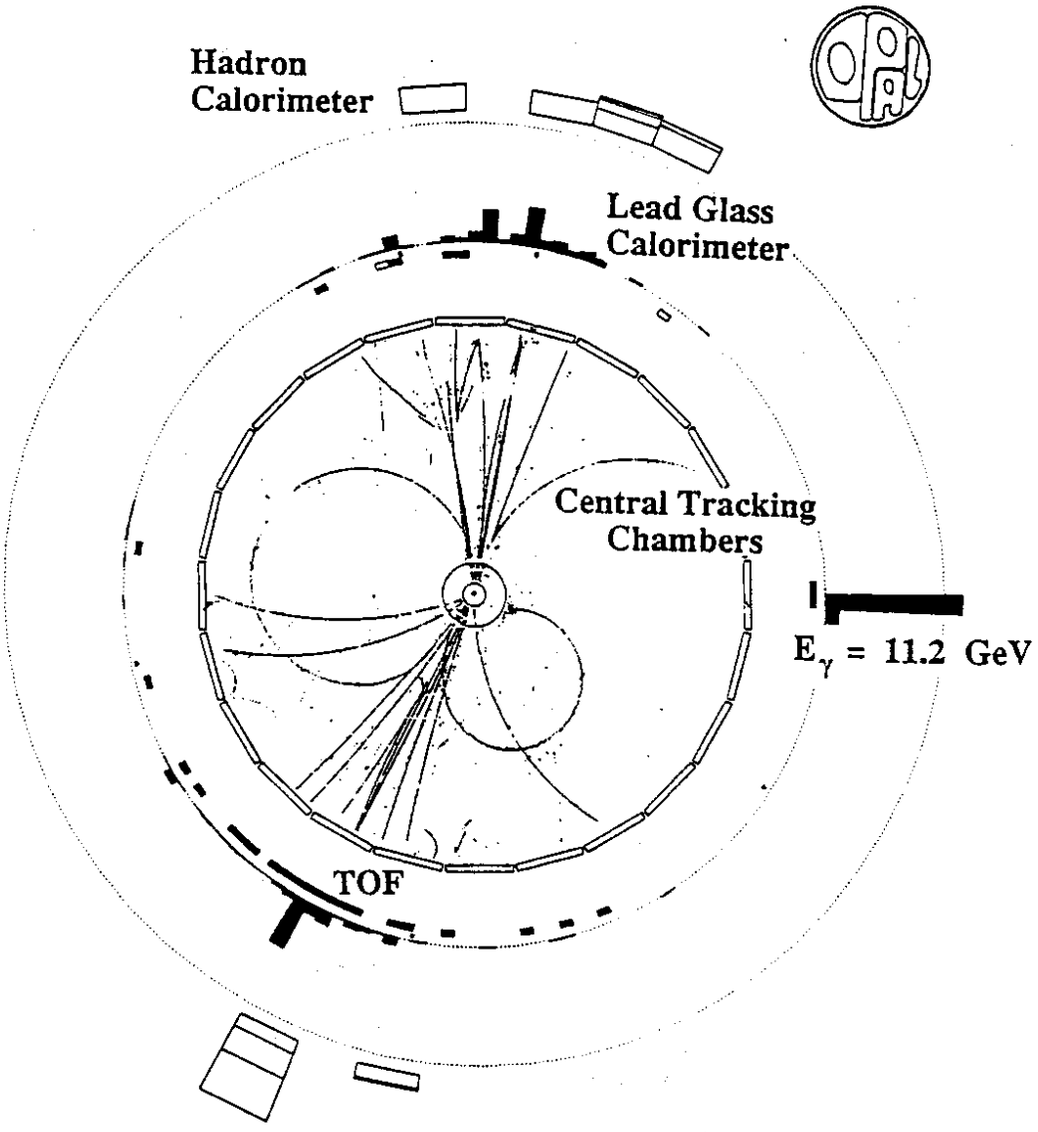
Hadron
Calorimeter
Lead Glass
Calorimeter
Central Tracking
Chambers
TOF
E_γ = 11.2 GeV

Figure 2

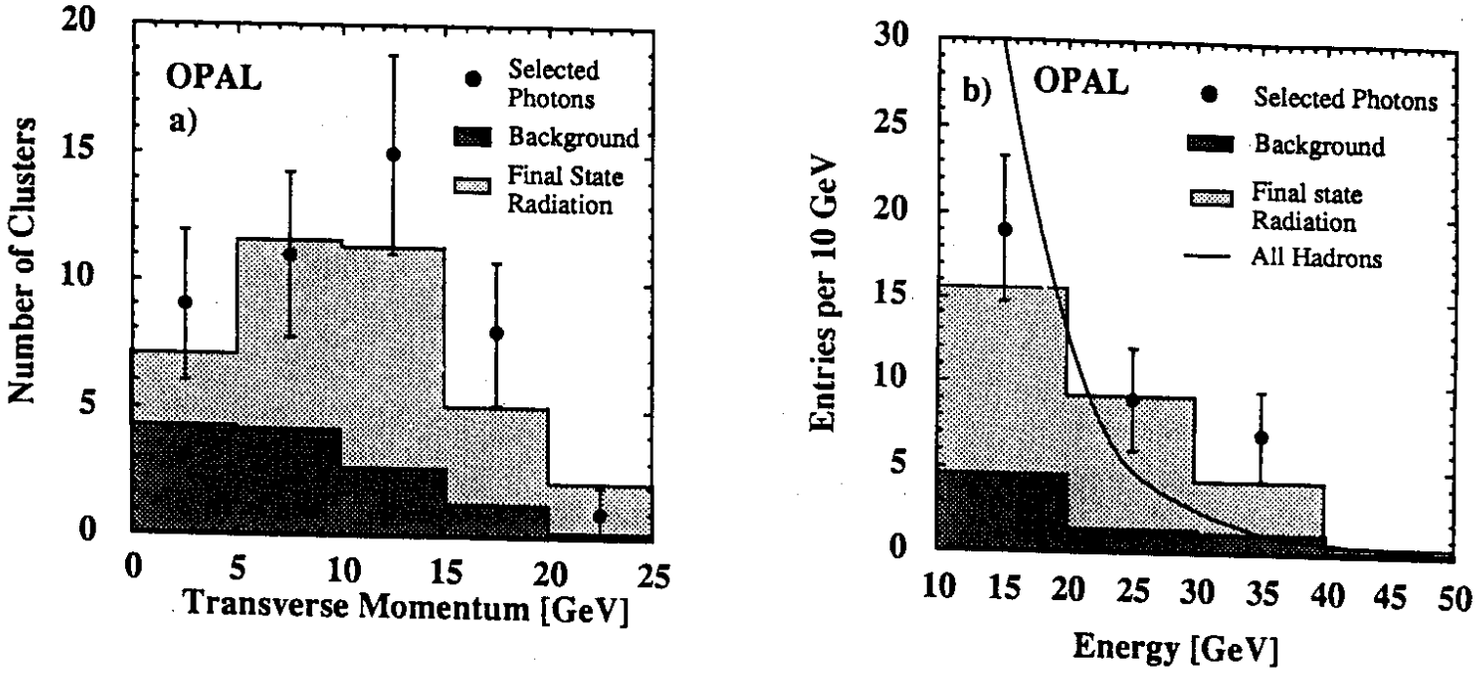

Figure 3

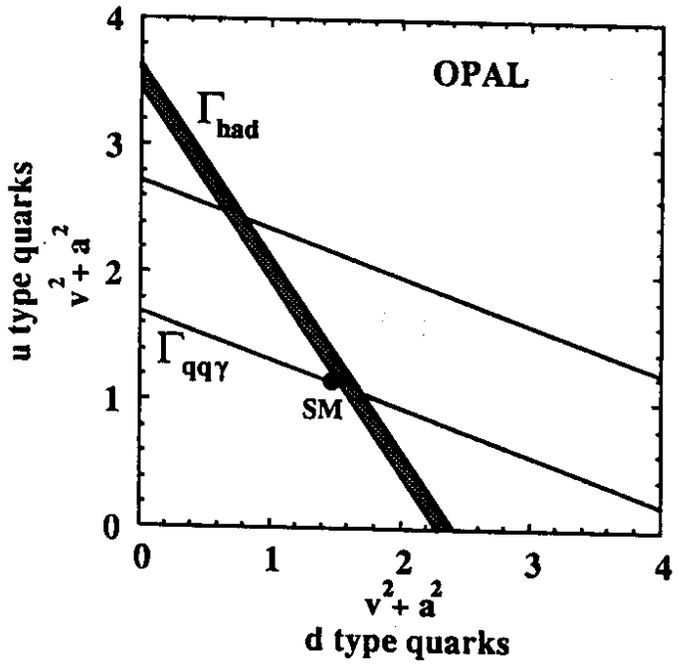

Figure 4

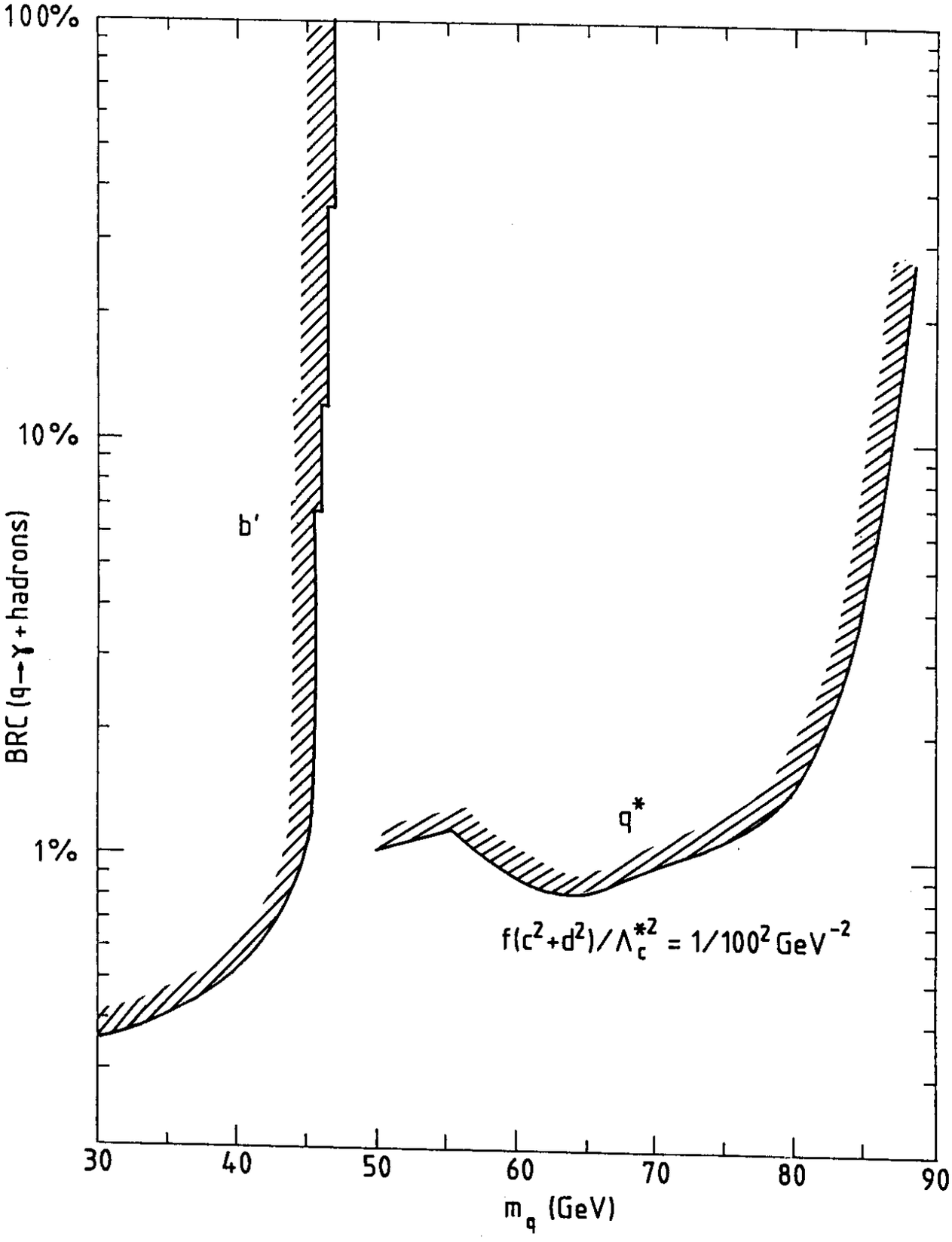
100%
10%
1%
BRC (q→γ+hadrons)
b'
q*
$f(c^2+d^2)/\Lambda_c^{*2} = 1/100^2\ GeV^{-2}$
30
40
50
60
70
80
90
m_q (GeV)

Figure 5